Eur. Phys. J. B **3**, 179–183 (1998)

THE EUROPEAN PHYSICAL JOURNAL B

Anharmonic behaviour of BaFCl using Raman scattering

B. Sundarakkannan[a] and R. Kesavamoorthy

Materials Science Division, Indira Gandhi Centre for Atomic Research, Kalpakkam-603 102, India

Received: 12 May 1997 / Accepted: 25 July 1997

Abstract. Raman scattering from oriented single crystals of BaFCl was recorded at various temperatures from 20 to 1073 K for the first time. The Raman spectra, corrected for phonon population, were fitted to the sum of four Lorentzian peaks. The peak frequencies and full width at half maximum (FWHM) of the peaks were obtained from the fit. The FWHM is accounted for by cubic and quartic anharmonic processes. The quartic anharmonicity of the mode increases with the mode frequency. The quartic anharmonicity of the fluorine mode is exceptionally high. The peak frequencies decrease linearly with the increasing temperature. Fluorine mode frequencies decrease more than the internal mode frequencies do. The LO-TO splitting of the fluorine modes and that of the internal modes increases with temperature indicating the increase of the ionic bonding character. The results are discussed.

PACS. 78.30.-j Infrared and Raman spectra – 63.20.-e Phonos in crystal lattices

1 Introduction

MFX (M = Ca, Sr, Ba; X = Cl, Br, I) ternary compounds, belonging to the matlockite structure (PbFCl), crystallize with tetragonal P4/nmm (D_{4h}^7) symmetry and platelet morphology. Planes containing all F ions, M ions and X ions are stacked one over the other along the c-axis in the sequence of F, M, X, X, M and F. MFX have a natural cleavage plane perpendicular to the c-axis where bonding between the neighbouring X-planes is weaker [1]. The growth rate along the a-axis is at least twenty times larger than that along the c-axis [2]. Single crystals of MFX are grown by flux method [3], Bridgman method [4], and modified Kyropoulos method [2]. It is reported that thick single crystals of MFX can be obtained in horizontal Bridgman growth by mixing MF_2 and MX_2 in stoichiometrically F–rich proportion [5]. In the modified Kyropoulos method thicker crystals can be grown using a ring heater around the growth interface but they tend to have a lot of inclusions [2]. The flux method yields high quality single crystals of relatively low thickness. However, dendritic growth was observed in such crystals [3,6].

Polarized Raman scattering from oriented MFX single crystals at room temperature has been recorded and the modes have been assigned [7]. The group theoretical analysis indicates the division of 18 degrees of freedom (2 molecules of MFX in the unit cell) into the modes of the following symmetries [7,8]

$$\Gamma_{18} = 2A_{1g} + B_{1g} + 3E_g + 3A_{2u} + 3E_u. \qquad (1)$$

There are six Raman active modes, namely, $2A_{1g}$, B_{1g} and $3E_g$. All of them appear in the unpolarized Raman spectra recorded with the ac-face oriented perpendicular to the incident beam. The Raman frequencies have been calculated and compared with the experimental values [9,10]. Infrared modes have been investigated in these crystals [6, 9]. Extensive lattice dynamics calculations have been carried out to obtain phonon dispersion relations, elastic constants, phonon density of states and specific heats of these crystals [10–12]. Ultrasonic and Brillouin scattering measurements [13] and cohesive energy calculations [14] confirm the predominantly ionic nature of the bonds, which is a basic input to the phonon calculations [10–12]. High pressure X-ray diffraction from BaFCl reveals a structural phase transition at about 21 GPa [15]. However, the high pressure phase has not yet been identified. High temperature X-ray diffraction (HTXRD) from BaFCl powder from 298 to 873 K has provided the thermal expansion coefficients of BaFCl [16]. HTXRD investigation of BaFCl single crystal from 298 to 883 K has provided the temperature dependence of the cell parameters and fractional coordinates [17]. Anharmonic potential parameters and anisotropic thermal vibration parameters of all the ions have also been obtained [17]. Electrical properties of alkaline earth fluorohalide (MFX) crystals have been investigated at high temperatures [18]. Ayachour *et al.* [18] have conjectured the possibility of an order-disorder type antiferroelectric to paraelectric phase transition at about 1000 K in BaFBr and BaFI based on dielectric measurements. However, they have not made mention of any phase transition in BaFCl. Ionic conductivity of BaFCl has been studied from 298 to 773 K [19].

In this work, the unpolarised Raman spectra of BaFCl single crystals oriented with their ac-face perpendicular to the incident beam were recorded from 20 to 1073 K and

[a] e-mail: suka%msd@igcar.ernet.in

analysed. The full width at half maximum (FWHM) and the peak frequency were obtained from the spectra. The results are discussed.

2 Experimental

Clear, transparent and dendrite-free single crystals of BaFCl ($5\times5\times0.5$ mm^3) were grown by the flux method. To grow single crystals of BaFCl, the powders of $BaCl_2.2H_2O$ and KF (both LOBA GR grade) were mixed in equal mole fraction and ground thoroughly in a mortar and pestle. The XRD pattern of the mixture showed the presence of BaFCl and KCl, indicating that reaction occurs while grinding itself. This mixed powder was loaded in a platinum crucible and heated to 1133 K in a vertical kanthal-wound muffle furnace where BaFCl dissolves in the molten KCl. The solution was cooled at a rate of 20 K/h till 973 K and then furnace cooled to RT (298 K). Methanol was used to separate out the single crystals from KCl matrix. Optical microscopic examination revealed that the crystals are clear, transparent and dendrite-free. The Laue pattern of the single crystal of BaFCl recorded at RT with c-axis parallel to the unfiltered Cu radiation X-ray beam in a Laue camera (Huber Type 802) indicates a strain-free single crystal nature [16,20]. The XRD pattern of the powdered BaFCl crystals obtained in a SIEMENS D-500 powder diffractometer using Cu$-K_\alpha$ radiation matched well with the ICDD pattern 240096 [16,20,21].

The unpolarized Raman spectra of BaFCl single crystals oriented with their ac-face perpendicular to the incident beam were recorded in a laser-Raman spectrometer built around a double grating monochromator, SPEX model 14018. A Kr-ion laser, lasing at 482.5 nm with 80 mW power was used as the source. This beam, after passing through a plasma filter [22], was focussed onto the oriented single crystal of BaFCl and the scattered light in the backscattering geometry was collected using a camera lens (Nikkon) and a focussing lens. A thermoelectrically cooled photomultiplier tube model ITT-FW 130 was used to detect the scattered light after passing through the monochromator. A microprocessor based automated data collection system was used. A slit width of the monochromator corresponding to 4.2 cm^{-1} in terms of FWHM of the instrument resolution function was employed. The scattered light was integrated for 5 S and digitally recorded at 0.5 cm^{-1} wavenumber interval.

Raman spectra were recorded in the range of 298 to 1073 K by heating the crystal in an one-end-closed cylindrical kanthal heater (3.5 cm internal dia., 5 cm length) which was controlled using a temperature controller, model INDOTHERM 401. The laser beam entered and the scattered light exited through the open-end of the heater. The sample was held in the heater by two 'L' shaped SS-strips. A K-type thermocouple was fixed near the sample. The temperature accuracy was about $\pm$ 1 K at temperatures below 573 K and about $\pm$ 2 K for higher temperatures.

Raman spectra were recorded in the range of 20 to 298 K in another laser Raman spectrometer using a closed cycle refrigeration system (Displex bought from M/s. Air Products, USA). An Ar^+ laser, lasing at 514.5 nm with 25 mW was used as the incident beam. A home-made double grating monochromator was employed along with a thermoelectrically cooled PMT [23]. The scattered light was integrated for 1 S for the low temperature measurements and digitally recorded at 0.5 cm^{-1} interval. The FWHM of the instrumental resolution function was 2.5 cm^{-1}.

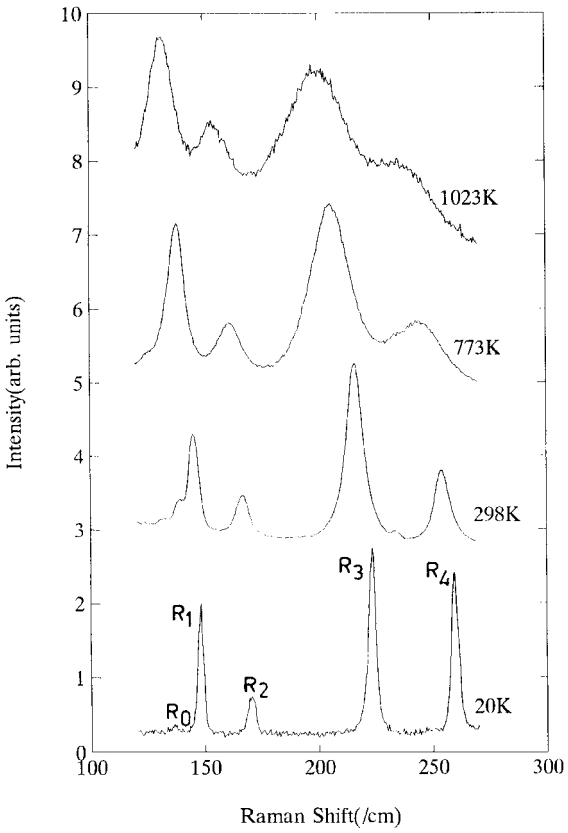

Fig. 1. The recorded unpolarised Raman spectra of BaFCl oriented single crystal at temperatures 20, 298, 773 and 1023 K. The Raman modes R_0, R_1, R_2, R_3 and R_4 are marked. The spectra were shifted from one another along Y-axis for clarity.

3 Results and discussion

Figure 1 shows the unpolarized Raman spectra of BaFCl single crystal oriented with their ac-face perpendicular to the incident beam at 20, 298, 773 and 1023 K. The high intensity Raman peaks at 145 (R_1), 167 (R_2), 216 (R_3) and 254 cm^{-1} (R_4) are marked in Figure 1. The low intensity Raman peak at 133 cm^{-1} (R_0) is also marked. R_0 belongs to A_{1g} external mode. R_1 and R_2 belong to E_g and A_{1g} internal Ba-Cl stretching modes respectively [7]. R_3 and R_4 belong to B_{1g} and E_g fluorine modes respectively [7]. The Raman spectrum was also recorded in the frequency range of 70 to 120 cm^{-1} and a weak peak was identified at about 82 cm^{-1}. This peak belongs to E_g external mode. This 82 cm^{-1} peak and R_0 were very weak to extract the information about the mode parameters. Hence R_1, R_2,

R_3 and R_4 were considered for the analysis. The red shift and broadening of the peaks with increasing temperature are clearly illustrated in this figure. The small humps seen at 137 and 232 cm^{-1} in the 298 K spectrum in Figure 1 are the plasma lines.

The Raman spectra were corrected for the phonon population density by dividing the recorded intensity by $1+n(\omega)$ where

$$n(\omega) = \left[\exp\left(\frac{\hbar\omega}{k_B T}\right) - 1\right]^{-1} \quad (2)$$

is the population factor [24]. Here, ω is the Raman frequency, T is the temperature, h is the Planck's constant and k_B is the Boltzmann constant. The corrected Raman spectrum, $I_c(\omega)$, was least square fitted to the sum of four Lorentzians centered at the peak frequencies, ω_{0i}, having the observed FWHM, Γ_{ei}, and a second order polynomial for the background intensity, namely,

$$I_c(\omega) = \sum_{i=1}^{4} a_{ei} \frac{\Gamma_{ei}^2}{\Gamma_{ei}^2 + (\omega - \omega_{0i})^2} + a_5 + a_6\omega + a_7\omega^2 \quad (3)$$

a_{ei} are the observed height of the Raman peaks. The fit was excellent and the parameters (ω_{0i} and Γ_{ei}) were considered for further analysis. Since the recorded Raman spectrum is a convolution of the actual spectrum and the instrumental resolution function having FWHM (Γ_s) of 4.2 cm^{-1} for high temperature spectra and 2.5 cm^{-1} for the low temperature spectra, the FWHM (Γ_{ei}) obtained from the fit using equation (3) would be different from the actual values. The true FWHM (Γ_i) were deduced from the observed values using the empirical relation given by Arora and Umadevi [25]. They convoluted the Lorentzian Raman line shape function having various Γ with the Gaussian spectrometer resolution function having various Γ_s by computation and obtained Γ_e of the convoluted function. They obtained empirical formula for Γ in terms of Γ_s and Γ_e which correctly reproduced the Γ of the Raman line shape function for various Γ_s and the computed Γ_e. This empirical relation was found to be valid for $\Gamma_e/\Gamma_s \geq 1$, which is satisfied in the present study.

Figure 2 shows the FWHM, Γ_i, of the four Raman modes as a function of temperature. Consider the Γ of any particular Raman mode. Γ increases monotonically with T. The temperature behaviour of Γ is analysed by considering the multiphonon processes. The cubic anharmonicity of the mode leads to the decay of a phonon of frequency ω_0 at temperature T into two phonons each of frequency $\omega_0/2$. These phonons would be longitudinal acoustic (LA) phonons [26]. This process results in the broadening of the Raman mode by [24,27]

$$\Gamma_c = A\left[\left(\exp\left(\frac{\hbar\omega_0}{2k_B T}\right) - 1\right)^{-1} + \frac{1}{2}\right] \quad (4)$$

where A is the constant. Similarly, the quartic anharmonicity leads to the decay of the phonon having the frequency ω_0 at temperature T into three phonons each of frequency $\omega_0/3$. These also would be LA phonons. This process results in the broadening by [24,28]

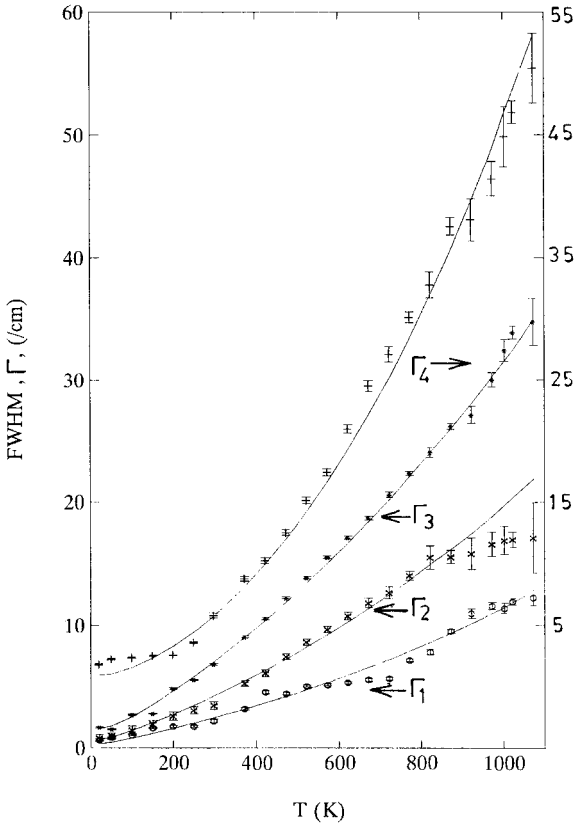

Fig. 2. Full width at half maximum, Γ_1(o), Γ_2(x), Γ_3(∗), and Γ_4(+) of the R_1, R_2, R_3 and R_4 modes as a function of temperature. The solid lines are the fit to the equation (6).

$$\Gamma_q = B\left[\left(\left(\exp\left(\frac{\hbar\omega_0}{3k_B T}\right) - 1\right)^{-1} + \frac{1}{2}\right)^2 + \frac{1}{12}\right], \quad (5)$$

where B is the constant. Γ is fitted to

$$\Gamma = \Gamma_c + \Gamma_q. \quad (6)$$

The solid lines in Figure 2 are the fits to equation (6). The fit are very good. The fitted values of A and B for all the modes are tabulated in Table 1. The values of B increases monotonically with the mode frequency, ω_0. This is expected since the dissipation of the vibrational energy *via* a four phonon process will be more important for a mode of higher frequency [24]. The value of B/A for R_4 is very large as compared to that for the other three Raman modes (Tab. 1). This might be due to the possibility that the R_4 mode phonon of frequency 254 cm^{-1} can decay into 3 phonons of frequency each of 84 cm^{-1} which happens to be the E_g external mode in the present system. This additional mode of decay, in addition to the decay into 3 LA phonons, might result in the larger quartic anharmonicity. The increase in Γ, when T is increased from 20 to 1073 K ($\Delta\Gamma$), shows a monotonic increase with ω_0 (Tab. 1).

Table 1. The values of the parameters A and B, of the fit to Γ (Eq. (6)), the ratio B/A, the change in Γ and that in ω_0 on heating the BaFCl from 20 to 1073 K, $\Delta\Gamma$ and $\Delta\omega_0$. $\Delta\Gamma = \Gamma(1073\text{ K}) - \Gamma(20\text{ K})$; $\Delta\omega_0 = \omega_0(20\text{ K}) - \omega_0(1073\text{ K})$.

Raman modes	Symbol used	Peak freq. at RT (cm^{-1})	A (cm^{-1})	B (cm^{-1})	B/A	$\Delta\Gamma$ (cm^{-1})	$\Delta\omega_0$ (cm^{-1})
E_g(int)	R_1	145	0.75	0.015	0.020	12	16
A_{1g}(int)	R_2	167	1.45	0.040	0.028	21	12
B_{1g}(flu)	R_3	216	3.2	0.085	0.027	33	23
E_g(flu)	R_4	254	1.6	0.490	0.306	52	21

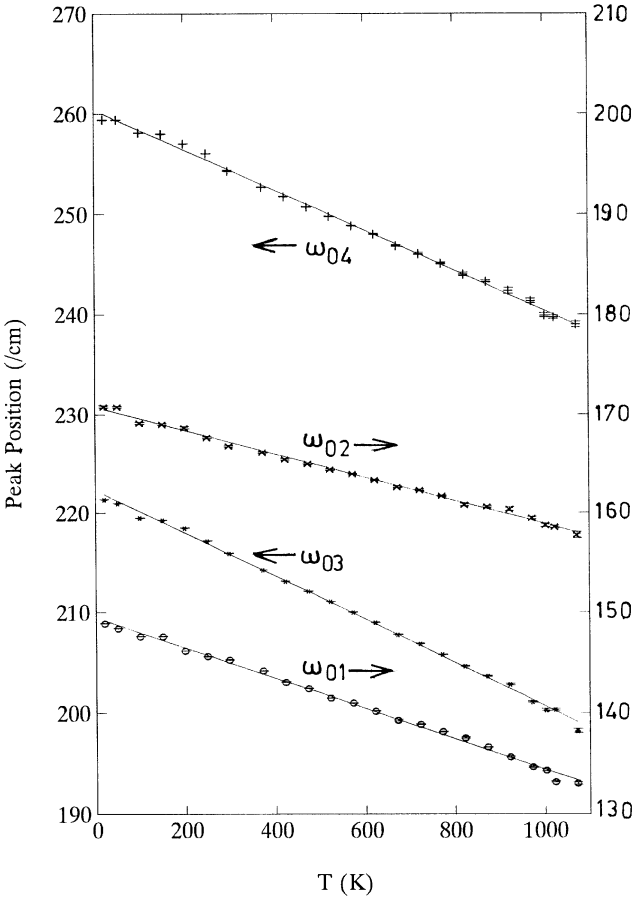

Fig. 3. The peak positions, ω_{01}(o), $\omega_{02}(\times)$, $\omega_{03}(*)$ and $\omega_{04}(+)$ of the Raman modes R_1, R_2, R_3 and R_4 as a function of temperature. The solid straight lines are the guide to the eye.

Figure 3 shows the temperature dependence of the peak positions of the four Raman modes. They decrease linearly with the increase of temperature from 20 to 1073 K. The solid straight lines are a guide to the eye. The change in peak position with temperature has resulted from quasi-harmonic contribution and anharmonic contribution [24]. The quasi-harmonic contribution can be understood in terms of thermal expansion and the resulting change of harmonic force constants. The anharmonic contribution arises due to the cubic and quartic anharmonicities [24,29]. In order to determine the quasi-harmonic contribution, the temperature dependences of the thermal expansion coefficients, molar volume, compressibility and the specific heat are required in the temperature region from 20 to 1073 K [24]. Though the first two data have been generated recently over a limited temperature region [16,17], the information about the other two are scanty. The calculated specfic heat data [11] has been shown to be incorrect [13]. Hence, the contributions to the change in peak position due to the various processes have not been calulated in this work. The decrease in ω_0 when T is increased from 20 to 1073 K ($\Delta\omega_0$) is given in Table 1. $\Delta\omega_0$ of the fluorine modes (R_3 and R_4) are larger than those of the internal modes (R_1 and R_2). This can be understood qualitatively on the basis of the recent report on the temperature dependence of the interionic separation distances in BaFCl [16]. The fluorine mode vibration involves predominantly the F–F separation distance while the internal mode vibration predominantly involves the Ba–Cl distance. When heated from 298 to 873 K, the F–F distance has increased by about 1.7% while the Ba–Cl distance increases by only about 0.3% [16]. As the bond length increases, the vibration frequency decreases due to the quasi-harmonic effect. Larger increase in the bond length implies a larger value of $\Delta\omega_0$. The cubic and quartic anharmonicity contribution to FWHM are larger for the fluorine modes as compared to those for internal modes (see Tab. 1). Anharmonicity also contributes to the decrease in the peak frequency. Fluorine modes have larger anharmonicities and hence the larger value of $\Delta\omega_0$. Hence, $\Delta\omega_0$ for fluorine modes can be expected to be more than that for internal modes.

It has been reported that the transverse optic (TO) branch of the internal Ba–Cl stretching mode occurs at 145 cm^{-1} and its longitudinal optic (LO) branch at 167 cm^{-1} at RT [7,8]. The frequency difference between these LO and TO (LO-TO splitting) is mainly due to the ionic bonding character. As the ionic character of the bond increases the LO-TO splitting will increase [30,31]. The fluorine mode also shows the LO-TO splitting. However, this splitting is inverted. Figure 4 shows the temperature dependence of the LO-TO splitting for the internal mode as well as for the fluorine mode. The solid straight lines are a guide to the eye. The LO-TO splitting for both the modes increases with the temperature indicating that the ionic character of the bonds increases with the temperature. As the bond lengths increase with temperature, the overlap of the electrons belonging to the bonding ions decreases and hence the increase of the ionicity.

There is no disappearance of a peak or appearance of a new peak in the Raman spectra with temperature. Further, the data presented here did not show any discontinuity in the temperature range of 20 to 1073 K indicating

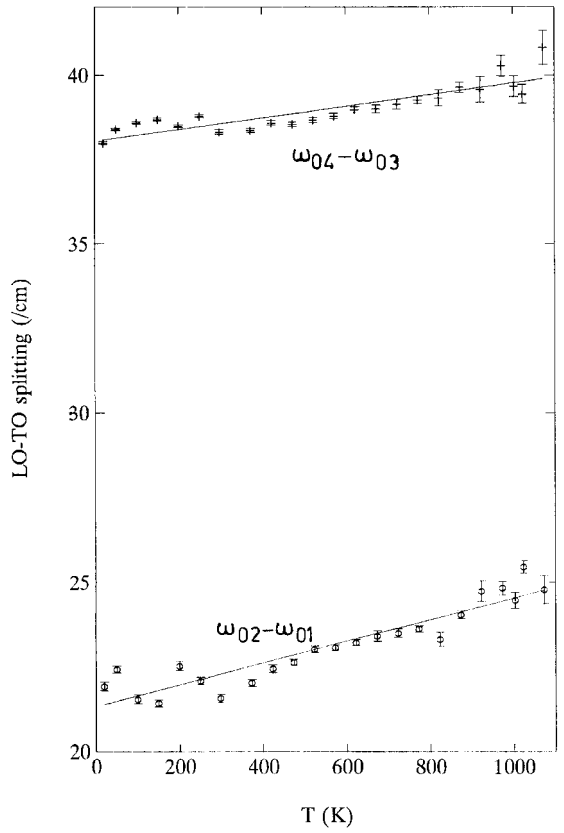

Fig. 4. The temperature behaviour of the LO-TO splitting of the fluorine modes (+) and that of the internal modes (o). The solid straight lines are the guide to the eye.

that there is no structural phase transition in BaFCl in this temperature range. The frequency of the E_g external mode was found to decrease from 84 cm^{-1} at 20 K to 71 cm^{-1} at 1073 K and that of A_{1g} external mode decreased from 136 cm^{-1} at 20 K to 118 cm^{-1} at 1073 K continuously. However, the error was large ($\pm$ 1 cm^{-1}) due to the low intensity of the modes.

4 Summary

Transparent and dendrite-free single crystals of BaFCl were grown by the flux method. Unpolarised Raman spectra from the oriented single crystal of BaFCl with *ac*-face perpendicular to the incident beam were recorded from 20 to 1073 K. The FWHM, Γ, of the peaks increases with temperature due to the cubic and quartic anharmonicities. The peak position decreases linearly with the increasing temperature. The faster decrease of the fluorine mode frequency than the internal mode frequency as T increases is understood on the basis of their corresponding increase in bond lengths with temperature and the anharmonicity of the modes. The LO-TO splitting of the modes increases with temperature indicating the increase of the ionic bonding character. There is no structural phase transition in the temperature range from 20 to 1073 K.

We thank Dr. S.K. Deb, BARC for providing us the low temperature Laser-Raman Spectrometer.

References

1. R. Sauvage, Acta Crystallogr. **B 30**, 2786 (1974).
2. E. Nicklaus, F. Fischer, J. Crystal Growth **12**, 337 (1972).
3. K. Somaiah, V. Hari Babu, Ind. J. Pure Appl. Phys. **14**, 702 (1976).
4. Y.R. Shen, T. Gregorian, W.B. Holzapfel, High Press. Res. **7**, 73 (1991).
5. K. Takahashi, J. Miyahara, J. Electrochem. Soc. **132**, 1492 (1985).
6. H.L. Bhat, M.R. Srinivasan, S.R. Girisha, A.H. Rama Rao, P.S. Narayanan, Ind. J. Pure Appl. Phys. **15**, 74 (1977).
7. J.F. Scott, J. Chem. Phys. **49**, 2766 (1968).
8. D. Nicollin, H. Bill, J. Phys. C Solid state phys. **11**, 4803 (1978).
9. L. Marculescu, Chem. Phys. Lett. **21**, 342 (1978).
10. K.R. Balasubramanian, T.M. Haridasan, N. Krishnamurthy, Solid State Commun. **32**, 1095 (1979).
11. K.R. Balasubramanian, T.M. Haridasan, J. Phys. Chem. Solids **42**, 667 (1981).
12. K.R. Balasubramanian, T.M. Haridasan, N. Krishnamurthy, Chem. Phys. Lett. **67**, 530 (1979).
13. M. Fischer, M. Sieskind, A. Polian, A. Lahmar, J. Phys. Cond. Matter **5**, 2749 (1993).
14. P. Herzig, J. Solid State Chem. **57**, 379 (1985).
15. Y.R. Shen, U. Englisch, L. Chudinovskikh, F. Porsch, R. Haberkorn, H.P. Beck, W.B. Holzapfel, J. Phys. Cond. Matter **6**, 3197 (1994).
16. R. Kesavamoorthy, B. Sundarakkannan, G.V. Narasimha Rao, V. Sankara Sastry, Thermochimica Acta **307**, 185 (1997).
17. N. Kodama, K. Tanaka, T. Utsunomiya, Y. Hoshino, F. Marumo, Solid State Ionics **14**, 17 (1984).
18. D. Ayachour, M. Sieskind, P. Geist, Phys. Status Solidi (b) **166**, 43 (1991).
19. K. Somaiah, V. Hari Babu, Ind. J. Pure App. Phys. **16**, 49 (1978).
20. B. Sundarakkannan, R. Kesavamoorthy, G.V. Narasimha Rao, in *Fundamentals of crystal growth* (Anna University, Madras, 1996), edited by R. Dhanasekaran, C. Subramanian, S. Moorthy Babu, p. 185.
21. B. Sundarakkannan, R. Kesavamoorthy, G.V. Narasimha Rao, in *Luminescence and its applications*, edited by S. Selvasekarapandian, P. Christoberselvan (Allied Publishers Ltd, Madras, 1996), p. 349.
22. T. Sakuntala, A.K. Arora, J. Meas. Sci. Tech. **4**, 596 (1993).
23. A.P. Roy, M.L. Bansel, Ind. J. Pure Appl. Phys. **26**, 218 (1988).
24. A.K. Sood, A.K. Arora, V. Umadevi, G. Venkataraman, Pramana **16**, 1 (1981).
25. A.K. Arora, V. Umadevi, App. Spectroscopy **36**, 424 (1982).
26. S. Safran, B. Lax, J. Phys. Chem. Solids **36**, 753 (1975).
27. K. Park, Phys. Lett. A **25**, 490 (1967).
28. T. Sakurai, T. Sato, Phys. Rev. B **4**, 583 (1971).
29. G. Leibfried, J. Phys. Chem. Sol. Suppl. **1**, 237 (1965).
30. J.F. Scott, Phys. Rev. B **4**, 1360 (1971).
31. F. Gevais, J.L. Servoin, J. Phys. France **42**, C6-415 (1981).